

We are IntechOpen, the world's leading publisher of Open Access books Built by scientists, for scientists

6,900

Open access books available

186,000

International authors and editors

200M

Downloads

Our authors are among the

154

Countries delivered to

TOP 1%

most cited scientists

12.2%

Contributors from top 500 universities



WEB OF SCIENCE™

Selection of our books indexed in the Book Citation Index
in Web of Science™ Core Collection (BKCI)

Interested in publishing with us?
Contact book.department@intechopen.com

Numbers displayed above are based on latest data collected.
For more information visit www.intechopen.com



Hydrothermal Conversion of South African Coal Fly Ash into Pure Phase Zeolite Na-P1

Mugera W. Gitari, Leslie F. Petrik and
Nicholas M. Musyoka

Additional information is available at the end of the chapter

<http://dx.doi.org/10.5772/63399>

Abstract

South African coal combustion power utilities generate huge amounts of coal fly ash that can be beneficiated into zeolitic products. This chapter reports on the optimization of the presynthesis and synthesis conditions for a pure-phase zeolite Na-P1 from selected South African coal fly ashes. The hydrothermal treatment time, temperature, and molar quantities of water during the hydrothermal treatment step were successfully optimized. The optimum hydrothermal treatment time and temperature were 48 h and 140°C, respectively. Pure-phase zeolite Na-P1 was obtained with a molar regime of 1 SiO₂:0.36 Al₂O₃:0.59 NaOH:0.49 H₂O at an aging temperature of 47°C for 48 h. The optimized conditions were applied to two fly ashes from two coal-fired power utilities, and high-purity zeolite Na-P1 was obtained. The third coal fly ash with a different chemical composition gave a low-quality Na-P1 under the optimized conditions. The cation exchange capacity for the high-purity zeolite phase was 4.11 mEq/g, indicating that the adjustment of reactant composition and presynthesis or synthesis parameters leads to yields of high-quality zeolite Na-P1. The results also show that conversion of the coal fly ash into high-purity zeolite also depends on the chemical and mineralogical composition of the coal fly ash.

Keywords: zeolite Na-P1, coal fly ash, hydrothermal synthesis, optimization, aging step, CEC

1. Introduction

South Africa relies mainly on coal combustion for power generation [1]. Low-grade bituminous coal is combusted for power generation; this in turn generates huge volumes of waste

materials such as bottom ash, fly ash, boiler slag, flue gas desulfurization sludge, and noncaptured particles [1, 2]. Of most concern is fly ash, which is mainly collected from flue gases by means of mechanical devices [3, 4]. After collection, fly ash is hydraulically transported to holding ponds, lagoons, landfills, and slag heaps, where it can be reacquired for treatment purposes or discarded or conveyed to ash heaps in dry disposal systems. The disposal and management of the huge quantities of coal fly ash has been a concern to industrial environmental managers and the scientific community and are in constant search for bulky beneficial utilization of coal fly ash to offset management costs and protect the environment. Approximately 27 Mt of fly ash is produced annually in South African power utilities [1]. Of this, only 5% is utilized beneficially. The remainder is discarded in surface impoundments, such as ash retention dams, where it continues to evolve chemically and mineralogically with possible environmental impacts [5]. Several researchers have proposed strategies for bulky utilization of fly ash, which include (i) applications as an additive in the manufacturing of cement, concrete, construction materials, and road pavements [6, 7], (ii) utilization of fly ash in zeolite synthesis for wastewater treatment [8–14], and (iii) use of fly ash in the neutralization of acid mine drainage and mine backfill [1, 15]. Most of these approaches are an attempt to beneficially use coal fly ash to supplement the cost of disposal and management and to reduce the negative environmental impact.

The application of coal fly ash in zeolite synthesis is of major interest due to the many industrial applications of zeolites, such as catalysis or catalyst carriers, adsorbents for the removal of inorganic and organic contaminants from wastewaters, management of radioactive wastes, gas separation, slow-release fertilizer, and in the manufacture of detergents [14]. The conversion of these low-cost waste products into products of higher value such as zeolites would allow the beneficiation of fly ash in an environment-friendly condition in addition to economic benefits. South African class F coal fly ash has been confirmed to be a good feedstock of Al and Si for zeolite synthesis because of its compositional dominance of aluminosilicate and silicate phases [14, 16]. Zeolite synthesis from fly ash is one of the potential environmentally useful applications of fly ash to produce high-value industrial products [10]. The major potential applications of zeolites synthesized from fly ash are based on their use as high capacity ion exchangers in industrial water waste treatment due to their large pore volumes [8, 10, 17]. Zeolites have also proven to be good candidates for use in soil decontamination [18] and have also shown great potential for use in the removal of postcombustion gases such as SO_x and NO_x [19].

Through various synthesis methods, researchers have synthesized various types of zeolites from fly ash, such as zeolite Na-P1 [20], zeolite A [21, 22], and zeolite ZSM-5 [23]. However, few studies have been successful in the conversion of fly ash into pure-phase zeolites [24]. Querol et al. [13] evaluated the synthesis of zeolites from fly ash at pilot scale using various Spanish fly ashes. The authors observed that, to obtain pure-phase zeolites, the optimum synthesis conditions have to be established for each coal fly ash. They attributed this to differences in mineralogical and chemical composition. South African coal fly ashes differ significantly in the chemical and mineralogical composition and this formed the basis of this work, as they have not been evaluated before as feedstocks to synthesize pure-phase zeolites.

The zeolite Na-P1 was chosen as the model zeolite to test our hypothesis. Zeolite Na-P1 belongs to an important group of zeolites that can be synthesized under mild hydrothermal synthesis conditions without using templates, making them potentially economically viable and a green product. The narrow particle size distribution of the zeolite Na-P1 coupled with the micron-sized crystallites and the unusual framework flexibility gives this zeolite unique, favorable ion exchange and water sorption properties [25]. Very few studies have reported on the synthesis of pure-phase zeolites, although numerous studies have been carried out in the synthesis of zeolites from coal fly ash using modified synthesis procedures [13, 21, 26]. Most of the studies have yielded low-quality zeolites due to the incomplete conversion of the coal fly ash matrix into zeolitic phase. Successful transformation of South African fly ash into impure zeolite P using the mild temperature method (100°C) was achieved by Petrik et al. [27].

Szostak [28] classified the factors affecting the zeolite crystallization as composition of the reaction matrix, time of reaction, temperature, and history-dependent factors such as stirring, aging, nature of mixture, and order of mixing. Casci [29] observed that the variation of individual reaction components and reaction variables, such as reaction temperature, alkaline concentration, and time of synthesis, influence the type of zeolite synthesized, the quality of the zeolite, and also the efficiency of the synthesis process. To achieve the complete dissolution of coal fly ash matrix and conversion into the zeolitic phase, the modification of presynthesis steps and synthesis and postsynthesis conditions is recommended. A two-step synthesis procedure developed by Hollman et al. was adapted for our optimization procedures using South African coal fly ashes [30]. The optimized parameters were hydrothermal treatment time, temperature, and water content during hydrothermal treatment. This chapter reports on the successful conversion of South African coal fly ash into pure-phase Na-P1 zeolite.

2. Sampling and experimental procedures

2.1. Sample handling

Pulverized coal fly ashes were collected from the ash collection systems at three different coal power utilities in Mpumalanga, South Africa. These coal fly ashes were used as feedstock for the zeolite synthesis. The sampled coal fly ash was stored in tightly locked plastic containers to prevent the ingress of moisture and CO₂ and out of direct sunlight. Coal fly ash consists of metastable phases and reactive components, which were formed during high-temperature combustion, and they are likely to react with CO₂ and moisture in the atmosphere forming new products. This might alter the chemical and mineralogical composition of the coal fly ash [30].

2.2. Synthesis procedures and equipment

A two-step process for the synthesis of zeolites from fly ash adopted from Hollman et al. [11] was followed, whereby a mixture of coal fly ash and alkaline solution was subjected to (1) aging and (2) hydrothermal treatment.

The setup for the aging process is shown in **Figure 1**. In this aging step, coal fly ash was mixed with sodium hydroxide (NaOH) pellets in a ratio of 1:1. The NaOH pellets were first dissolved in 100 mL ultra-pure water in a separate beaker and then added to the coal fly ash in a 250 mL HDPC temperature-resistant sealable bottle, and a magnetic bar was added and the mixture in the sealed bottle was then heated on a magnetic stirrer hotplate. The hotplate was adjusted to a predetermined temperature of 47°C, which was controlled by a temperature probe, while the speed of rotation was set at 800 rpm. The aging temperature and time were kept constant at 47°C and 48 h, respectively, as reported from a previous study [27], to be optimum for the dissolution of aluminosilicate matrix of the coal fly ash in alkaline media.

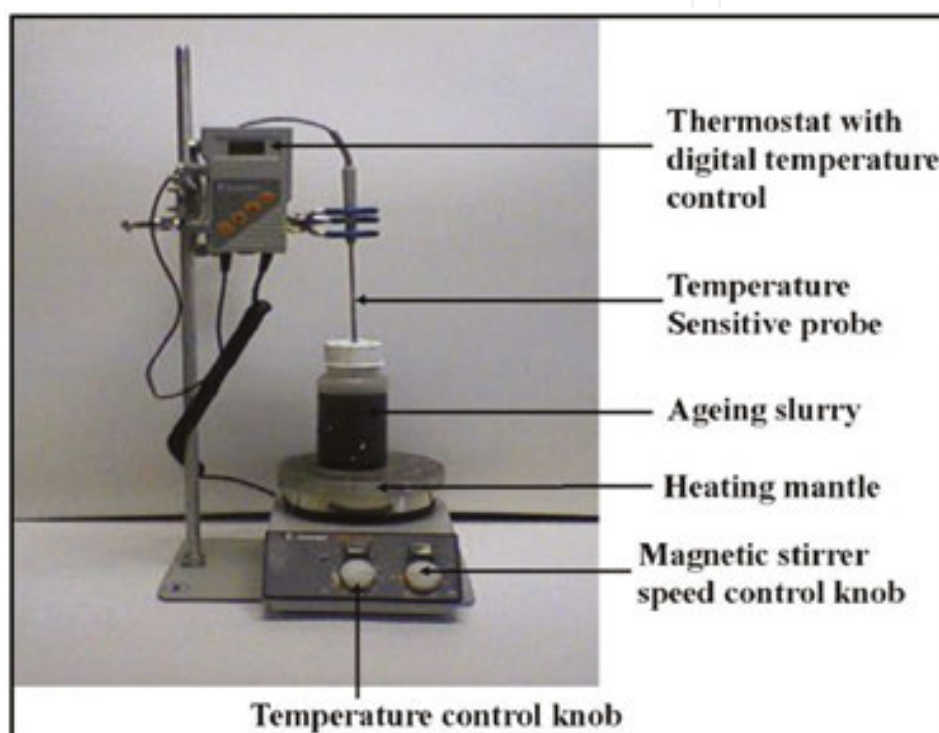


Figure 1. Experimental set-up for the aging process.

For hydrothermal treatment, varying amounts of ultra-pure water were added to the slurry after aging, the mixture was stirred, and the resulting homogenous solution was transferred in aliquots of 10 mL into a 23 mL Parr bomb. The crystallization of the feedstock was achieved by placing the mixture in sealed Parr bombs in a thermostated Memmert hot air oven for a predetermined time and temperature (100–160°C at intervals of 20°C with parallel time variation of between 12 and 48 h at intervals of 12 h).

After hydrothermal treatment at the predetermined time and temperature, the sample bearing Parr bombs were removed from the oven and allowed to cool down to room temperature. The cooled mixture was filtered to obtain the filtrates and the solid residue products. The pH of the filtrate was determined, whereas the solid product was washed thoroughly with ultra-pure water until the washing attained a pH of 9 to 10. The supernatant solution was acidified and

kept refrigerated until analysis for chemical species. When the pH of the rinse solution had reached 9, the phases were separated and the solid product was recovered and dried overnight at 90°C and then transferred into airtight plastic containers before characterization. The pH and EC of solutions and supernatants were measured using HANNA HI 991301 portable pH/EC/TDS/temperature meter, which was calibrated before taking the measurements.

2.3. Characterization

The chemical composition of the coal fly ash and the synthesized zeolitic materials was carried out using X-ray fluorescence spectroscopy (XRF; Philips PW 1480 X-ray spectrometer). The samples were prepared by mixing 9 g of coal fly ash or zeolitic material with 2 g of a binder (10% C-wax binder and 90% EMU powder). The mixture was then thoroughly shaken, poured into the mould, and pelletized at a pressure of 15 tons for ~1 min using a Dickie and Stockler manual pelletizer. Loss on ignition (LOI) was measured by placing the samples in the furnace at 1000°C for at least 45 min. The instrument operating conditions for major element analysis were on a fused glass bead at 40 kV and 50 mA tube, whereas those for trace species were on a powder briquette at 50 kV and 40 mA tube operating conditions.

The samples for X-ray diffraction (XRD) were ground to a fine powder. The qualitative and quantitative XRD analyses of the coal fly ash and synthesized zeolite samples were done by placing the powder samples in a sample holder. The sample pattern was generated by a Philips X-ray diffractometer with Cu K α radiation. The crystalline phases were identified by matching the obtained XRD profile with the powder diffraction file data (Joint Committee of Powder Diffraction Standards) files for inorganic compounds. The quantification of crystalline and amorphous phases was done as follows: After the addition of 20% Si (Aldrich; 99% purity) for the determination of amorphous content, the samples were milled in a McCrone micronizing mill. XRD profiles were acquired with a PANalytical X'Pert Pro powder diffractometer with X'Celerator detector and variable divergence and receiving slits with Fe filtered Co K α radiation generated at 20 mA and 40 kV. The phases were identified using X'Pert Highscore Plus software. The relative phase amounts (wt.%) were estimated using the Rietveld method (Autoquan Program).

The morphology of the coal fly ash and the zeolitic products were examined using a scanning electron microscope (Hitachi X-650, Tokyo, Japan) with a compact detecting unit lead detector at 25 kV. The samples were mounted on aluminum pegs and sput coated with a thin film of gold for conductivity. For analysis by transmission electron microscopy (TEM), the samples were prepared by diluting a suspension of the synthesis products in ethanol, ultrasonicing, and depositing a drop onto S147-4 Holey carbon film 400 mesh Cu grids. A 200 kV field emission gun lens 1 was used with spouts size 3 at 200 kV using high-resolution TEM (HRTEM) Tecnai G2 F20 XTwin MAT.

The cation exchange capacity (CEC) was determined following the methods of Amrhein et al. [31]. The untreated coal fly ash was first saturated through three repeated rinsing steps with 1.0 M sodium acetate (pH 8.2) followed by four washings with ultra-pure water. The extraction of the exchangeable cations was done with three aliquots of 1.0 M ammonium acetate (pH 8.2). A 0.5 g of the zeolitic products was extracted in succession with four 25 mL aliquots of 1.0 M

ammonium acetate (pH 8.2). On the addition of the 25 mL extracting solution, the mixture was then continuously agitated for 15 min, centrifuged for 15 min, and decanted. The procedure was repeated four times and the cumulative extract was collected for each sample. The concentrations of exchangeable cations (Na^+ , Mg^{2+} , Ca^{2+} , and K^+) in the final solution were determined by inductively coupled plasma-atomic emission spectrometry. The CEC was then reported as mEq/g sample.

The surface area and pore size determination of the zeolitic products were carried out using the Brunauer-Emmett-Teller (N₂-BET) surface analysis technique. The samples (0.35–0.5 g) were first outgassed at 110°C using helium gas. Micromeritics Tristar instrument (Tristar3000, Micromeritics, Norcross, GA, USA) was used with nitrogen as the analysis gas based on a 5 point with 30 adsorption and 30 desorption points.

3. Results and discussion

3.1. Characterization of coal fly ash and zeolitic products

The chemical composition of the coal fly ash feedstock and the zeolitic products reported as oxides is presented in **Table 1**.

Chemical component	Coal fly ash A (% w/w)	Coal fly ash B (% w/w)	Coal fly ash C (% w/w)	Zeolite A (% w/w)	Zeolite B (% w/w)	Zeolite C (% w/w)
SiO ₂	50.91	49.79	54.92	36.69	35.16	33.95
Al ₂ O ₃	30.91	31.75	27.27	25.17	22.57	31.81
Fe ₂ O ₃	3.46	3.17	4.78	2.28	1.78	2.28
MnO	0.02	0.00	0.05	0.06	0.04	0.04
MgO	1.48	0.98	1.07	2.21	1.48	1.12
CaO	6.2	4.62	3.69	6.07	4.36	3.65
Na ₂ O	0.10	0.09	0.07	6.53	9.17	5.49
K ₂ O	0.60	0.63	0.66	0.13	0.13	0.14
P ₂ O ₅	0.56	0.67	0.61	0.04	0.06	0.04
TiO ₂	1.65	1.46	0.3	1.58	1.24	1.95
SO ₃	0.24	0.23	1.71	0.06	0.06	0.03
LOI	3.85	6.59	4.44	11.92	13.91	10.99
Total	99.99	99.98	99.58	99.81	98.2	99.21
SiO ₂ /Al ₂ O ₃	1.65	1.57	2.01	1.45	1.56	1.07

Table 1. Chemical composition of coal fly ash and synthesized zeolites.

For all coal fly ash feedstock, the $\text{SiO}_2 + \text{Al}_2\text{O}_3 + \text{Fe}_2\text{O}_3$ is $\geq 70\%$, meaning the fly ashes can be classified as class F fly ash (ATSM method C 618). This is consistent with coal fly ash from the combustion of bituminous coal from South Africa [32]. The LOI ranged from 3.85% to 6.59% (w/w). LOI represents the unburned carbon in coal fly ash. The mean $\text{SiO}_2/\text{Al}_2\text{O}_3$ ratio ranged from 1.65 for coal fly ash A, 1.57 for B, and 2.01 for C. The $\text{SiO}_2/\text{Al}_2\text{O}_3$ ratio is important in that it directly governs both the Si/Al ratio of the zeolite product and the incorporation of Al in the framework structure. The presence of CaO and MgO plays a significant role in zeolite synthesis. The Ca^{2+} and Mg^{2+} ions act as competing cations during synthesis [33]. The lower content of CaO in coal fly ash C could result in the lower alkalinity of the solution during aging and hydrothermal synthesis, which could affect the rate of depolymerization and monomerization process [33]. The $\text{SiO}_2/\text{Al}_2\text{O}_3$ for zeolite A (from coal fly ash A) was 1.45 less than in the feedstock fly ash, indicating the inefficient conversion of the feedstock. Na_2O was observed to be higher in all the zeolites compared to the feedstock; this is because of the incorporation of Na as a charge-balancing cation, as NaOH was used as the alkaline coal fly ash matrix dissolution agent.

The qualitative XRD results of coal fly ash A are presented in **Figure 2** (note that the XRD profile is similar for coal fly ashes B and C and hence not shown), whereas **Figure 3** shows a summary of the quantitative analysis of the three coal fly ashes.

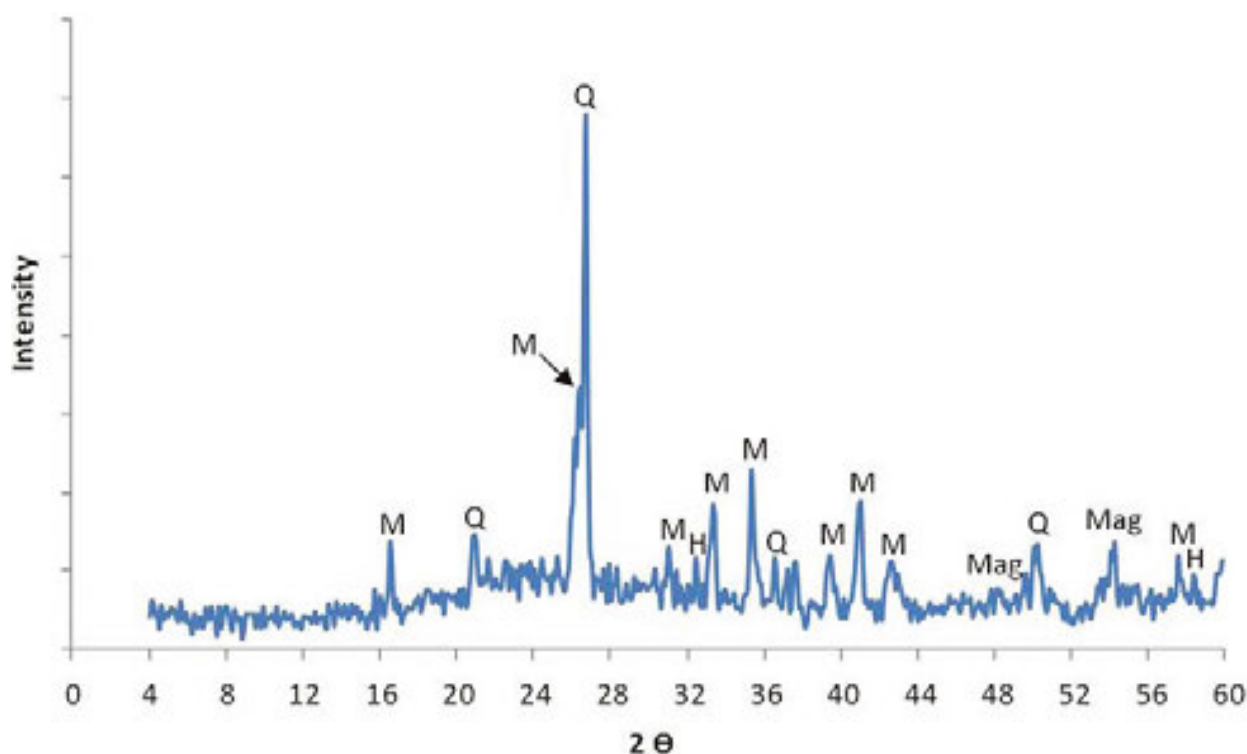


Figure 2. XRD profile of coal fly ash A (Q = quartz, M = mullite, H = hematite, Mag = magnetite).

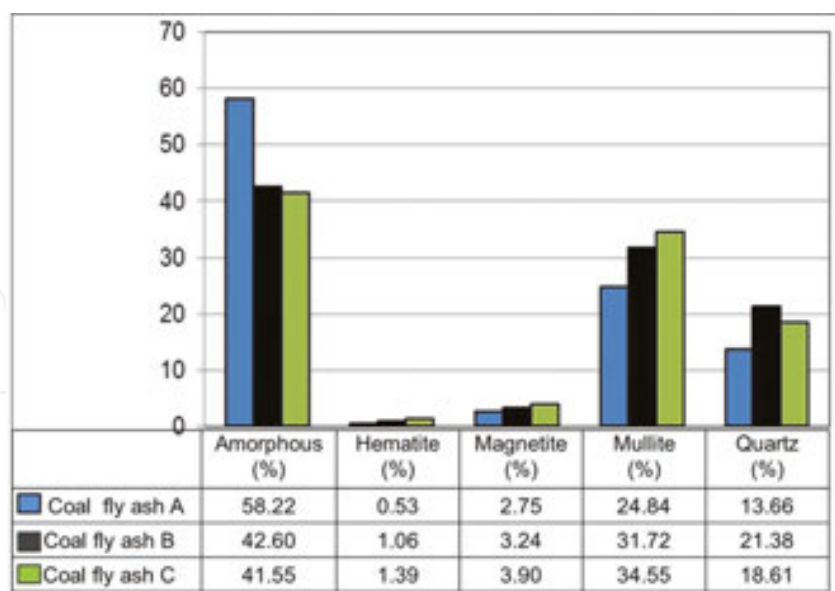


Figure 3. Relative quantitative XRD analysis of the three coal fly ashes.

The qualitative XRD analysis indicated the presence of the following mineral phases in all coal fly ash, quartz, mullite, magnetite, and hematite (**Figure 2**). The presence of the amorphous phase can be identified as the broad diffraction “hump” in the region between 18° and 32° 2θ [21, 26]. The quantitative analysis results show that mullite, quartz, and amorphous materials comprised 96% of the total mineral composition (**Figure 3**). It is noticeable in **Figure 3** that coal fly ash A has a higher content of the amorphous phase and the lowest quantity of quartz, mullite, hematite, and magnetite phases. Rayalu et al. [22] pointed out that the low levels of mullite promote zeolite synthesis and this is attributed to the fact that mullite is resistant to dissolution during hydrothermal treatment. The presence of the aluminosilicate phases in all the evaluated coal fly ashes qualifies their potential for the conversion to zeolite Na-P1.

3.2. Optimization of zeolite synthesis conditions

The optimization of the zeolite synthesis conditions was carried out using coal fly ash A. These optimized conditions were then applied for zeolite synthesis using coal fly ashes B and C and the properties of the zeolitic material compared to that resulting from coal fly ash A. The optimized conditions were the hydrothermal treatment temperature, time, and amount of water during the hydrothermal treatment process. The results are presented in terms of the chemical and mineralogical analysis of the zeolitic products, morphology, CEC, surface area, and pore volume.

3.2.1. Optimization of the hydrothermal treatment temperature and time

XRD was employed as a tool to monitor the evolution of zeolitic phases during the hydrothermal treatment process. Several authors pointed out that the increase of temperature leads to an increase in mullite dissolution, nucleation, and growth in zeolite crystals and an increased

in Si dissolution from coal fly ash leading to an increase in Si/Al ratio, which influences the crystallinity of the final zeolitic product [10, 33, 34]. **Figure 4** shows the XRD profile of zeolitic products for a concurrent variation of hydrothermal treatment time and temperature for coal fly ash A feedstock. **Figure 4a** shows the XRD profile of the transformation of different phases of the coal fly ash as a function of time at hydrothermal treatment temperature of 100°C. **Figure 4a** shows the disappearance of the broad hump between 18° and 32° 2θ (**Figure 2**), signifying the dissolution of the amorphous glassy phase during the hydrothermal treatment. The zeolitic phase produced was identified as zeolite Na-P1 ($\text{Na}_6\text{Al}_6\text{Si}_{10}\text{O}_{32}\cdot 12\text{H}_2\text{O}$). Some quartz, mullite, and hematite phases remained undissolved from the matrix even after 48 h hydrothermal treatment time at 100°C. **Figure 4b** shows the XRD profile of the transformation of different phases of the coal fly ash as a function of time at the hydrothermal treatment temperature of 120°C. The hydrothermal treatment at 120°C for various times did not result in pure-phase zeolite. An incomplete dissolution of the coal fly ash matrix was also observed with mullite and quartz being identified. However, a new zeolitic phase was identified as hydroxy-sodalite formed in all treatment times. At an increased hydrothermal treatment temperature of 140°C (**Figure 4c**), an increased dissolution of the coal fly ash aluminosilicate matrix was observed with increased hydrothermal treatment time, leading to almost complete dissolution at 48 h. The hematite mineral phase was completely dissolved. At 160°C hydrothermal treatment temperature, the mullite and quartz phases were gradually dissolved as the treatment time increased with complete dissolution at 48 h. However, another zeolitic phase was observed (hydroxyl-sodalite, whose peaks increased in intensity with increasing time; **Figure 4d**). The optimization of the hydrothermal treatment time and temperature identified

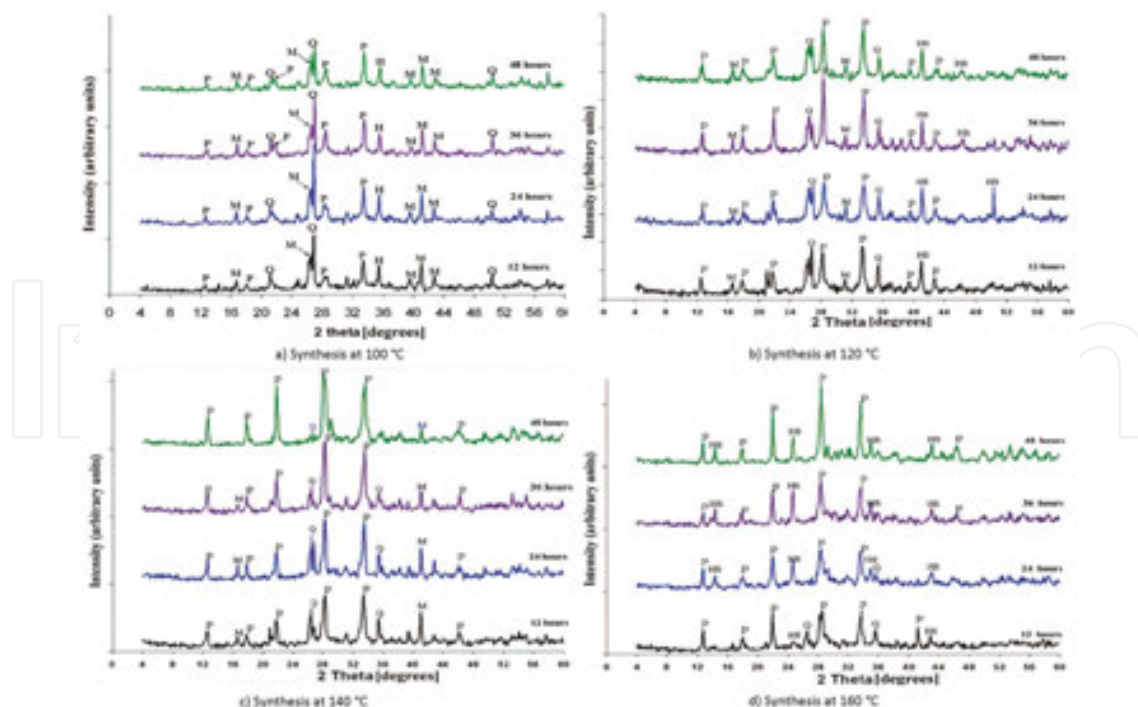


Figure 4. XRD profile of zeolitic products on the concurrent variation of hydrothermal treatment time (12–48 h) and temperature (100–160°C) for coal fly ash A (P = zeolite Na-P1, Q = quartz, M = mullite, H = hematite, HS = hydroxyl-sodalite). Reproduced with permission from Taylor & Francis Group, LLC, the copyright owners.

140°C temperature and 48 h as the optimum conditions for the synthesis of pure-phase zeolite Na-P1. However, traces of mullite and quartz were still observed in the almost pure phase obtained.

3.2.2. Effect of variation of water during hydrothermal treatment process

During the aging process, the dissolution of the aluminosilicate matrix of the coal fly ash occurs, releasing Si and Al, which are the main building blocks of the zeolite. Depending on the conditions employed, the saturation of the ionic precursors can occur, hindering more dissolution. The addition of water will tend to dilute the concentration of the ionic precursors leading to the further dissolution of the coal fly ash matrix. **Figure 5** shows the XRD profile of zeolitic products obtained on varying the water added during the hydrothermal treatment at 140°C and 48 h treatment time.

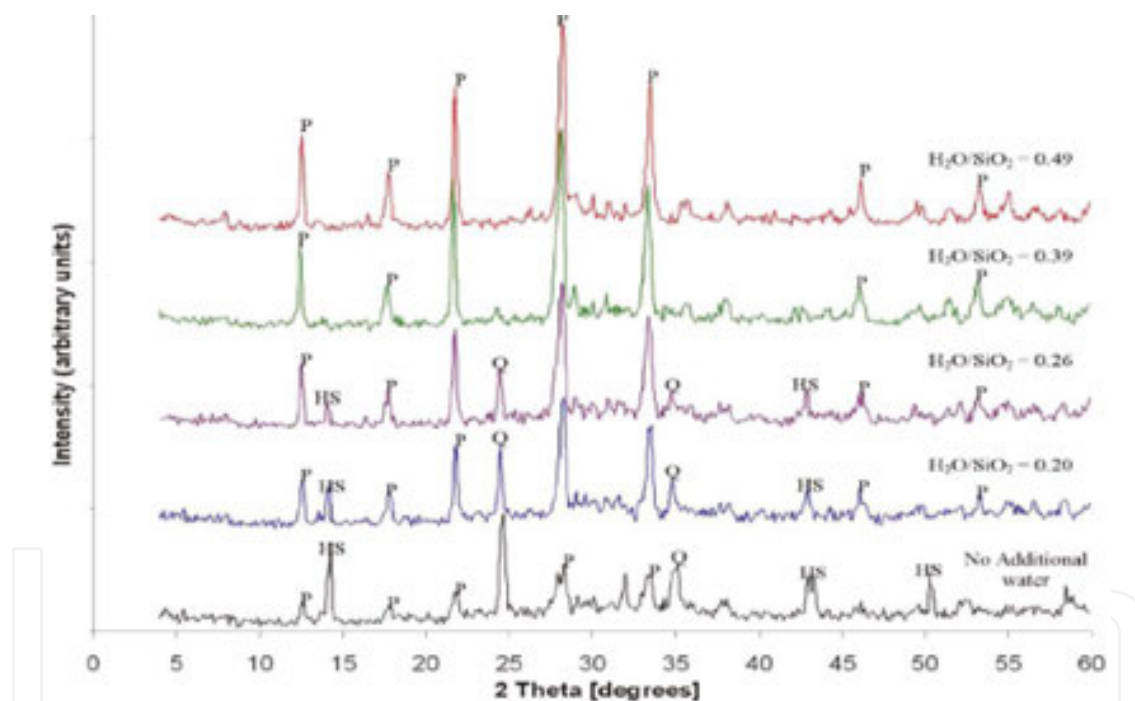


Figure 5. XRD profile of zeolitic products synthesized at 140°C for 48 h with variation of water during the hydrothermal treatment (P = zeolite Na-P1, HS = hydroxy-sodalite, Q = quartz). Reproduced with permission from Taylor & Francis Group, LLC, the copyright owners.

The additional water was added after the aging process, as equal amounts of water (100 mL) had been used during the aging process. It is observed that the addition of more water after aging enabled the formation of relatively pure phase of zeolite Na-P1. A balance has to be struck on the amount of water to be added, as too much water can also change the degree of supersaturation, which can slow the crystallization kinetics in addition to increasing the cost

of zeolite synthesis due to the need to manage the disposal of large amounts of effluent generated.

3.2.3. Relative percent crystallinity of the zeolitic products

The relative percent crystallinity of the zeolitic products was done by summing and normalizing the peak heights of five major peaks ($2\theta=12^\circ$, 23° , 28° , 33° , and 46° ; **Figure 4c**). The normalized peaks of zeolite Na-P1 synthesized at 140°C for 48 h was assumed to be 100% crystalline for the purpose of comparing to the spectra of the zeolites synthesized at 12, 24, and 36 h. A comparison of the percent crystallinity (peak heights) of the zeolite Na-P1 with quartz peaks was observed to be inversely proportional (**Figure 6**). This suggested the dissolution of quartz phase and the release of Si, which was then made available for the zeolitization.

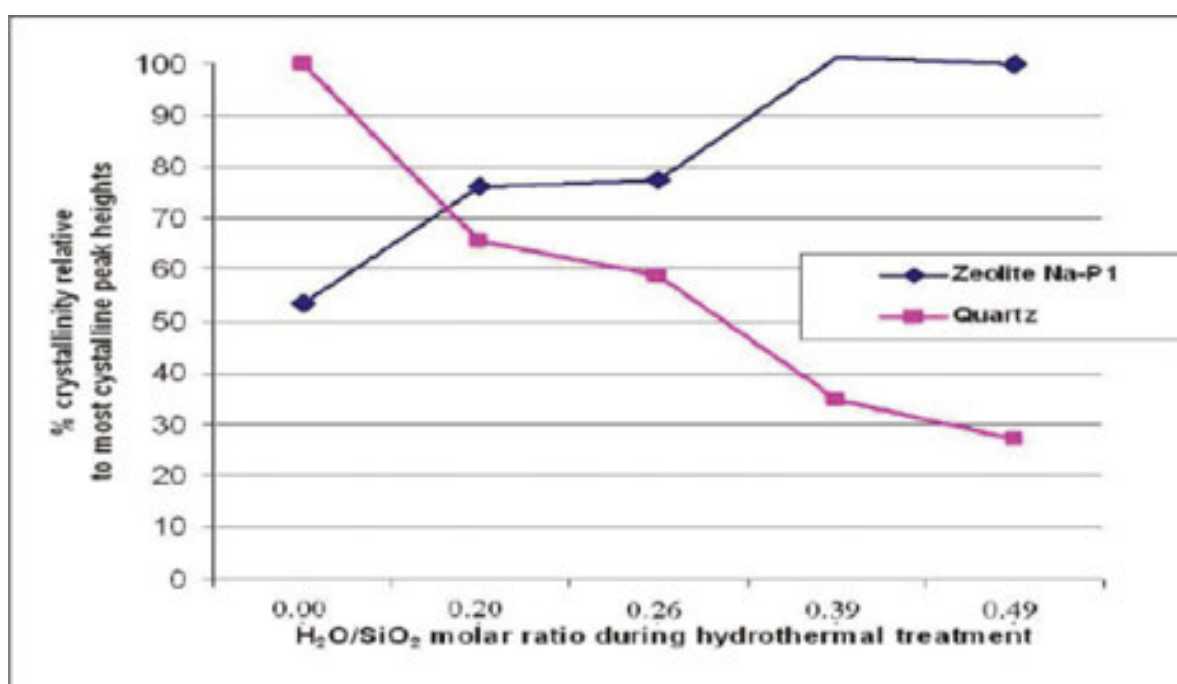


Figure 6. Comparison of the relative percent crystallinity of quartz and zeolite Na-P1 synthesized at 140°C (48 h) by varying the $\text{H}_2\text{O}/\text{SiO}_2$ molar ratio during the hydrothermal treatment.

3.3. Synthesis of zeolite Na-P1 using other coal fly ashes at optimized conditions

To test the success of the optimization process, the synthesis of zeolite Na-P1 from different coal fly ash feedstock was attempted at the optimized conditions. The XRD and XRF characterization of these coal fly ashes (coal fly ashes B and C) were presented previously (**Figures 2 and 3; Table 1**). **Figure 7** presents a comparison of the XRD profile of zeolite Na-P1 synthesized from coal fly ashes A, B, and C at the previously optimized conditions (140°C hydrothermal temperature and 48 h treatment time). **Figure 7** indicates that the zeolite Na-P1 produced with coal fly ash B was similar to that of coal fly ash A. However, coal fly ash C showed an incomplete dissolution of mullite and quartz. This could be attributed to the

difference in chemical and mineralogical composition of the coal fly ash C compared to coal fly ashes A and B (Figures 2 and 3; Table 1). This indicates that the conditions employed were not optimum for the dissolution of quartz and mullite in coal fly ash C. Another observable fact about the incomplete zeolitization of coal fly ash C could be due to the low CaO, which is known to contribute to the alkalinity of the solution. Coal fly ash C had the lowest CaO content (Table 1).

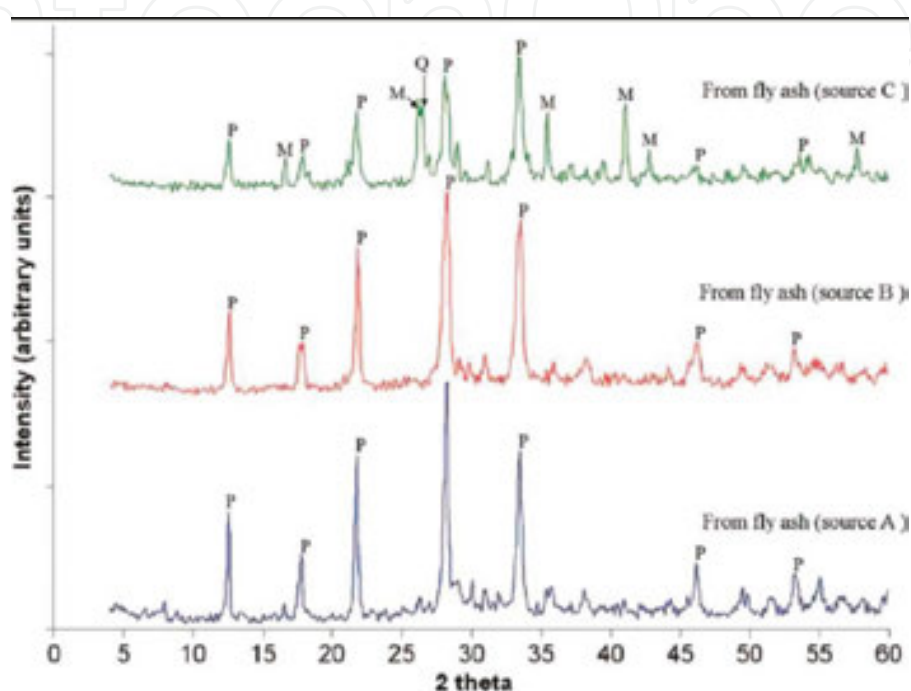


Figure 7. XRD profile of zeolites synthesized from coal fly ashes A, B, and C at 140°C and 48 h treatment time. Reproduced with permission from Taylor & Francis Group, LLC, the copyright owners.

3.4. Morphological evolution of the coal fly ashes during the synthesis process

The morphological evolution of the coal fly ash feedstock after aging and hydrothermal treatment is depicted in Figure 8. The coal fly ash has a smooth spherical appearance and typically consists of microspheres. Gitari et al. [15] have previously reported the smooth spherical appearance of South African coal fly ash. The coal fly ash particles are observed to be smooth spheres, as the glassy phase covers the particles. The coal fly ash after the aging process appears to show a partial disintegration of the spheres, indicating the conditions employed during aging are not sufficient to completely break the matrix. This could also point to the resistance of mullite and quartz to dissolution. However, after hydrothermal treatment, a transformation of the disintegrating microspheres was observed, with granular crystalline particles being observed on the surface of the spheres. These were identified by XRD to be the zeolitic phases. Walek et al. [24] reported that the hydrothermal crystallization process begins on the surface of the undissolved or partially dissolved coal fly ash particle. These granular particles represented the initial zeolite formation process. A further illustration of the evolution

of the crystalline zeolitic phases is depicted during the variation of water during the hydrothermal treatment at 140°C temperature for 48 h (Figure 9). Crystalline granules are clearly evident on the surface of the microspheres, which increases as the amount of water is increased. The crystallinity is also evident from the increasing agglomeration of the crystalline granules. The formation of the well-ordered crystalline zeolitic phase formed during aging conditions of 47°C for 48 h and hydrothermal treatment for 48 h at 140°C with H₂O/SiO₂ ratio of 0.49 was confirmed by use of HRTEM (Figure 10).

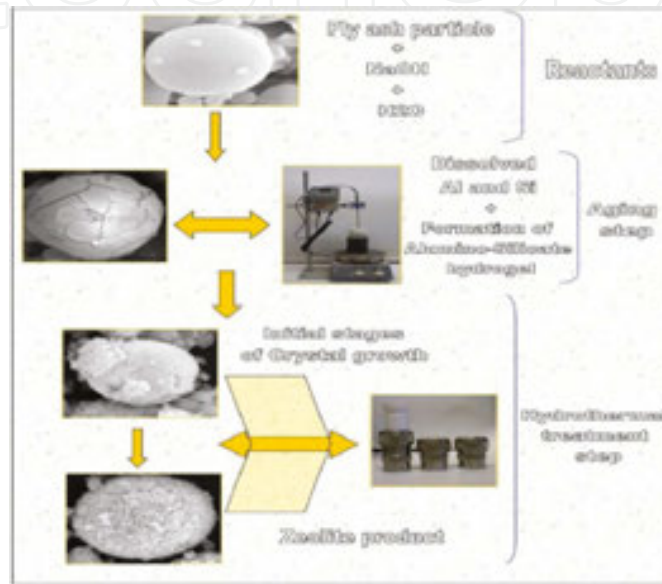


Figure 8. Morphological illustration of the reaction mechanism for the formation of zeolite phases.

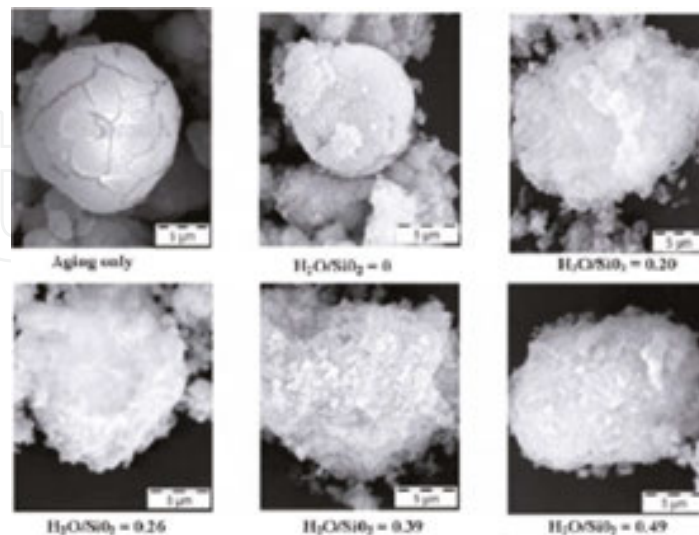


Figure 9. Morphological evolution of the zeolitic phases with variation of water content during the hydrothermal treatment.

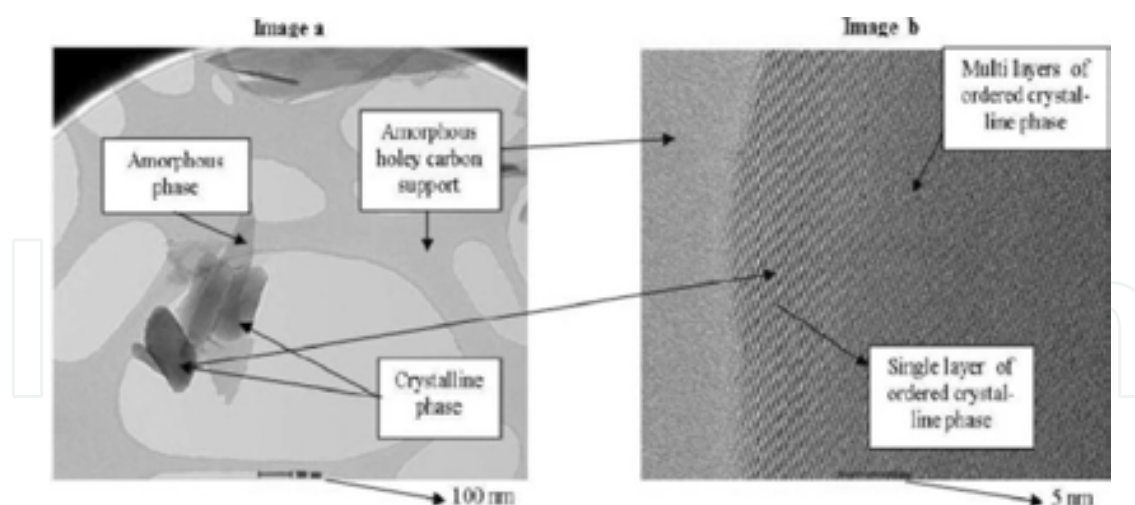


Figure 10. HRTEM micrograph showing the well-ordered crystalline zeolitic phase obtained from coal fly ash A feedstock.

In conclusion, the observations on the morphological transformation/evolution of the coal fly ash indicate that the glassy phase was dissolved in alkaline media and subsequently transformed into zeolite crystals, which were deposited on the surface of the disintegrating microsphere. The zeolite formation mechanism can therefore be described as (1) the dissolution of the SiO_2 and Al_2O_3 from the glassy phase/mullite/quartz in alkaline media, (2) the formation of aluminosilicate gel as zeolite precursor from SiO_4 and AlO_4 species, and (3) the crystallization of the zeolite phase at supersaturation of the alkaline media. The addition of water during hydrothermal treatment lowers the supersaturation and allows more dissolution of the glassy phase/mullite/quartz and the release of more SiO_4 and AlO_4 species leading to increased formation of the zeolite phase. The disintegration of the fly ash microsphere is predicted to continue with increased dissolution of the resistant mullite and quartz phases, as more hydroxyl ions migrate through the microsphere with continued hydrothermal treatment and subsequent formation of crystalline zeolitic phases (**Figure 9**).

3.5. CEC and surface area

The CEC of the zeolitic products was determined to provide further evidence to the purity of the phases. An increase in CEC was observed in the zeolitic products compared to the feedstock coal fly ash. Coal fly ash had a CEC of 0.48 mEq/g, zeolite product at 100°C/48 h of 2.98 mEq/g, and zeolite product at 140°C/48 h of 3.91 to 4.11 mEq/g. These results correlate well with the increasing crystallinity observed in the optimization stages (**Figures 4** and **9**). The results also compare closely to the CEC value of commercial zeolite Na-P1 (5 mEq/g). The addition of water during the hydrothermal treatment enhanced the CEC of the zeolitic products (zeolitic product obtained at 140°C/48 h with a $\text{H}_2\text{O}/\text{SiO}_2$ molar ratio of 0.49 was 4.10 mEq/g). This again confirms the high crystallinity and purity of the zeolitic phase obtained at this synthesis conditions. The BET analysis of surface area showed that the surface area of the material obtained after aging was low (30.5693 m^2/g), but this was observed to increase significantly on hydrothermal treatment at 24 h/140°C (58.6358 m^2/g).

and 48 h/140°C (67.6329 m²/g), which again confirms the high-purity and crystallinity of the zeolitic phase.

4. Conclusions

South African coal fly ashes have been proven to be suitable feedstock for hydrothermal conversion into high-purity zeolite Na-P1. The compositional and mineralogical analysis of the South African coal fly ashes identified mineral phases quartz, mullite, and amorphous glassy phase, which acts as crucial ingredients for the zeolite synthesis process. The optimization of the hydrothermal treatment process identified the conditions for the synthesis of high-purity zeolite Na-P1 as molar regime of 1 SiO₂:0.36 Al₂O₃:0.59 NaOH:0.49 H₂O and synthesis conditions of aging slurry at 47°C for 48 h. This was followed by hydrothermal treatment at 48 h and 140°C. The addition of water after the aging step expressed as H₂O/SiO₂ molar ratio was observed to play an important role in the hydrothermal conversion of coal fly ash into high-purity zeolites. The results show that a simple adjustment of reactant composition and presynthesis or synthesis parameters leads to almost complete dissolution of coal fly ash matrix and the conversion of the Si/Al ionic precursors into high-purity zeolite Na-P1. The high purity and CEC (4.11 mEq/g) imply that the zeolites from the class F South African coal fly ash can meet high-end applications such as wastewater treatment or application in detergents.

Acknowledgements

The authors would like to acknowledge the Water Research Commission (WRC), National Research Foundation (NRF), and Coaltech 2020 for funding this research work.

Author details

Mugera W. Gitari^{1*}, Leslie F. Petrik² and Nicholas M. Musyoka³

*Address all correspondence to: mugera.gitari@univen.ac.za

1 Environmental Remediation and Water Pollution Chemistry Group, School of Environmental Sciences, University of Venda, Thohoyandou, South Africa

2 Environmental and Nano Science Research Group, Department of Chemistry, University of the Western Cape, Cape Town, South Africa

3 Materials Science and Manufacturing, Council for Scientific and Industrial Research, Pretoria, South Africa

References

- [1] Petrik LF, White R, Klink M, Somerset V, Key D, Iwuoha E, Burger C, Fey MV. Utilization of fly ash for acid mine drainage remediation. Pretoria, South Africa: Water Research Commission; 2005. 174 pp. ISBN: 1-77005-316-6
- [2] ESKOM Annual Report. 2010. Available at: www.eskom.co.za
- [3] ESKOM Annual Report. 2001. Available at: www.eskom.co.za
- [4] Gitari WM, Leslie FP, Key DL, Okujeni C. Partitioning of major and trace inorganic contaminants in fly ash acid mine drainage derived solid residues. *International Journal Environmental Science Technology*. 2010; 7: 519–534. ISSN: 1735-1472
- [5] Gitari WM, Fatoba OO, Leslie FP, Vadapalli VRK. Leaching characteristics of selected South African fly ashes: Effect of pH on the release of major and trace species. *Journal of Environmental Science and Health Part A*. 2009; 44: 206–220. DOI: 10.1080/10934520802539897
- [6] Molina A, Poole C. A comparative study using two methods to produce zeolites from fly ash. *Minerals Engineering*. 2004; 17: 167–173. DOI: 10.1016/j.mineng.2003.10.025
- [7] Ye Y, Zeng X, Qian W, Mingwen W. Synthesis of pure zeolites from supersaturated silicon and aluminium alkali extracts from fused fly ash. *Fuel*. 2008; 87: 1880–1886.
- [8] Holler H, Wirsching U. Zeolite formation from fly ash. *Fortschritte der Mineralogie*. 1985; 63: 21–43.
- [9] Shigemoto N, Hayashi H, Miyama K. Selective formation of Na-X zeolite from coal fly ash by fusion with sodium hydroxide prior to hydrothermal reaction. *Journal of Materials Science*. 1993; 17: 4781–4786. DOI: 10.1007/BF00414272
- [10] Querol X, Plana F, Alastuey A, López-Soler A. Synthesis of Na-zeolites from fly ash. *Fuel*. 1997; 76: 793–799. DOI: 10.1016/S0016-2361(96)00188-3
- [11] Hollman GG, Steenbruggen G, Janssen-Jurkovicová M. A two-step process for the synthesis of zeolites from fly ash. *Fuel*. 1999; 78: 1225–1230. DOI: 10.1016/S0016-2361(99)00030-7.
- [12] Woolard CD, Petrus K, Van der Horst M. The use of modified fly ash as a sorbent for lead. *Water SA*. 2000; 26: 531–536. ISSN: 0378-4738
- [13] Querol X, Umana F, Plana F, Alastuey A, López-soler A, Medinaceli A, Valero A, Domingo MJ, Garcia-rojo E. Synthesis of zeolites from fly ash at pilot scale. Example of potential applications. *Fuel*. 2001; 80: 857–865. DOI: 10.1016/S0016-2361(00)00156-3
- [14] Somerset VS, Petrik LF, White RA, Klink MJ, Key D, Iwuoha E. The use of X-ray fluorescence (XRF) analysis in predicting the alkaline hydrothermal conversion of fly

- ash precipitates into zeolites. *Talanta*. 2004; 64: 109–114. DOI: 10.1016/j.talanta.2003.10.059
- [15] Gitari MW, Petrik LF, Etchebes O, Key DL, Iwuoha E, Okujeni C. Treatment of acid mine drainage with fly ash, removal of major contaminants and trace elements. *Journal Environmental Science Health Part-A Toxicology Hazard Substances Environmental Engineering*. 2006; 41: 1729–1747. DOI: 10.1080/10934520600754425
- [16] Derkowski A, Franus W, Beran E, Czimerová A. Properties and potential applications of zeolitic materials produced from fly ash using simple method of synthesis. *Powder Technology*. 2006; 166: 47–54. DOI: 10.1016/j.powtec.2006.05.004
- [17] Flanigien EM. Zeolite and molecular sieves: A historical perspective. In: Van Bekkum H, Flanigen EM, Jansen JC, editors. *Introduction to Zeolite Science and Practice*. 2nd ed. Amsterdam, Netherlands: Elsevier Science; 1991. pp. 13–33. ISBN: 978-0-444-82421-9
- [18] Singer A, Berkgaut V. Cation exchange properties of hydrothermally treated coal fly ash. *Environmental Science and Technology*. 1995; 29: 1748–1753. DOI: 10.1021/es00007a009
- [19] Querol X, Moreno N, Umaña JC, Alastuey A, Hernández E, López-Soler A, Plana F. Synthesis of zeolites from fly ash: An overview. *International Journal of Coal Geology*. 2002; 50: 413–423. DOI: 10.1016/S0166-5162(02)00124-6
- [20] Inada M, Tsujimoto H, Eguchi Y, Enomoto N, Hojo J. Microwave assisted zeolite synthesis from fly ash in hydrothermal process. *Fuel*. 2005; 84: 1482–1486. DOI: 10.1016/j.fuel.2005.02.002
- [21] Murayama N, Yamamoto H, Shibata J. Mechanism of zeolite synthesis from fly ash by alkali hydrothermal reaction. *International Journal Mineral Processing*. 2002; 64: 1–17. DOI: 10.1016/S0301-7516(01)00046-1
- [22] Rayalu SS, Udhoji JS, Munshi KN, Hasan MZ. Highly crystalline zeolite—A from flyash of bituminous and lignite coal combustion. *Journal of Hazardous Materials*. 2001; 88: 107–121. DOI: 10.1016/S0304-3894(01)00296-5
- [23] Chareonpanich M, Namto T, Kongkachuichay P, Limtrakul J. Synthesis of ZSM-5 zeolite from lignite fly ash and rice husk ash. *Fuel Processing Technology*. 2004; 85: 1623–1634. DOI: 10.1016/j.fuproc.2003.10.026
- [24] Walek TT, Saito F, Zhang Q. The effects of low solid/liquid ratio on hydrothermal synthesis of zeolites from fly ash. *Fuel*. 2008; 87: 3194–3199. DOI: 10.1016/j.fuel.2008.06.006
- [25] Zholobenko VL, Dwyer J, Zhang R, Chapple AP, Rhodes NP, Stuart JA. Structural transitions in zeolite P. An in situ FTIR study. *Journal of Chemical Society*. 1998; 94: 1779–1781. DOI: 10.1039/A800060C

- [26] Hui KS, Chao CYH. Effects of step-change of synthesis temperature on synthesis of zeolite 4A from fly ash. *Microporous Mesoporous Materials*. 2005; 88: 145–151. DOI: 10.1016/j.micromeso.2005.09.005
- [27] Petrik LF, Hendricks N, Ellendt A, Burgers C. Toxic element removal from water using zeolite adsorbents made from solid waste residues. Pretoria, South Africa: Water Research Commission; 2007. 133 pp. ISBN: 1770054642, 9781770054646
- [28] Szostak R. Molecular sieves, principles of synthesis and identification. In: Van Nostrand Reinhold Catalysis Series. The Netherlands: Springer; 1989. DOI: 10.1007/978-94-010-9529-7
- [29] Casci JL. Zeolite molecular sieve: Preparation and scale up. *Microporous and Mesoporous Material*. 2005; 82: 217–226. DOI: 10.1016/j.micromeso.2005.01.035
- [30] Gitari MW, Petrik LF, Reynolds K. Chemical weathering in a hypersaline effluent irrigated dry ash dump: An insight from physicochemical and mineralogical analysis of drilled cores. *Energy Science and Technology*. 2011; 2: 43–55. DOI: 10.3968/j.est.1923847920110202.110
- [31] Amrhein C, Gaghnia GH, Kim TS, Mosher PA, Gagajena RC, Amanios T, Torre IDL. Synthesis and properties of zeolites from coal fly ash. *Environmental Science and Technology*. 1996; 30: 735–742. DOI: 10.1021/es940482c
- [32] Gitari M, Petrik LF, Key D, Etchebers O, Okujeni C. Mineralogy and trace element partitioning in coal fly ash/acid mine drainage co-disposed solid residues. In: *Proceedings of the World of Coal Ash Association Conference, Lexington, KY, USA; 11–15 April 2005*. pp. 1–21.
- [33] Catalfamo P, Pasquale SD, Corigliano F, Mavilia L. Influence of the calcium content on the coal fly ash features in some innovative applications. *Resources, Conservation and Recycling*. 1997; 20: 119–125. DOI: 10.1016/S0921-3449(97)00013-X
- [34] Feijen EJP, Martens JA, Jacobs PA. Zeolites and their mechanism of synthesis. In: *Proceedings of the 10th International Zeolite Conference, Garmisch-Partenkirchen, Germany; 17–22 July 1994*. pp. 3–21.